Presence of Specific ^{11}C-*meta*-Hydroxyephedrine Retention in Heart, Lung, Pancreas, and Brown Adipose Tissue

James T. Thackeray[1,2], Rob S. Beanlands[1,2], and Jean N. DaSilva[1,2]

[1]*Cardiovascular PET Molecular Imaging Program, National Cardiac PET Centre, Division of Cardiology, University of Ottawa Heart Institute, Ottawa, Ontario, Canada; and* [2]*Department of Cellular and Molecular Medicine, Faculty of Medicine, University of Ottawa, Ottawa, Ontario, Canada*

^{11}C-*meta*-Hydroxyephedrine (HED) is used in cardiac PET as an index of norepinephrine (NE) reuptake transporter (NET) density and synaptic NE levels. Whereas cardiac uptake is well documented, tracer retention in other tissues with rich noradrenergic innervation is unclear. Dysfunctional sympathetic nervous system (SNS) function in extracardiac metabolic storage tissues (i.e., adipose tissue and skeletal muscle) and endocrine organs contributes to several disorders. The aim of this study was to determine the potential of HED as an index of NE function in brown adipose tissue, lung, pancreas, skeletal muscle, and kidney by identifying NET-specific retention and determining the presence of radiolabeled metabolites. **Methods:** Male Sprague–Dawley rats were administered HED and sacrificed at 30 min after tracer injection. Tissues were rapidly excised and counted for radioactivity, and relative tracer retention was quantified. Pretreatment with NET inhibitors established specific HED accumulation. The effect of elevated NE was tested by subcutaneous minipump NE infusion or inhibition of monoamine oxidase. Column-switch high-performance liquid chromatography (HPLC) was used to analyze the presence of radiolabeled metabolites in heart, brown adipose tissue, pancreas, and plasma. **Results:** NET-specific retention was observed in heart, brown adipose tissue, lung, and pancreas but not in liver, skeletal muscle, or kidney. A dose-dependent response of HED accumulation to treatments elevating NE levels was established in tissues exhibiting specific uptake. At 30 min after tracer administration, HPLC analysis revealed 93%–95% of total radioactivity signal derived from unchanged HED in heart, pancreas, and brown adipose tissue compared with 61% ± 8% unchanged HED in plasma. **Conclusion:** In addition to the heart, lung, pancreas, and brown adipose tissue exhibit specific and NE-responsive uptake of HED, supporting the potential for novel PET studies of SNS integrity in these tissues.

Key Words: sympathetic nervous system function; norepinephrine transporter uptake-1; competition with norepinephrine; HPLC column-switch system

J Nucl Med 2007; 48:1733–1740
DOI: 10.2967/jnumed.107.043570

Received May 11, 2007; revision accepted Jul. 11, 2007.

For correspondence or reprints contact: Jean N. DaSilva, PhD, Cardiac PET Centre, University of Ottawa Heart Institute, 40 Ruskin St., Ottawa, Ontario, Canada, K1Y 4W7.
E-mail: jdasilva@ottawaheart.ca

The sympathetic nervous system (SNS) is a primary extrinsic control mechanism mediating cardiac function, metabolic processes, and adaptation to stress. In normal conditions, the neurotransmitter norepinephrine (NE) is released from the presynaptic bouton into the synapse, where it binds to and stimulates adrenoceptors on pre- and postsynaptic cells. Excess NE is recycled into the presynaptic neuron by active transport via the uptake-1 NE reuptake transporter (NET) (*1,2*).

In myocardium, the SNS modulates heart rate, cardiac output, and stroke volume (*2*). In metabolic storage tissues, SNS activation stimulates 2 key processes: lipolysis—the breakdown of lipids primarily in white adipocytes—and thermogenesis—the uncoupling of mitochondrial energetics promoting heat release over energy storage, primarily in brown adipocytes and skeletal muscle (*3*). The SNS also partially controls pancreatic secretion of insulin and glucagon, hormones that regulate energy homeostasis by promoting glucose packaging and liberation, respectively (*4*). A growing body of evidence suggests that SNS dysfunction may be concomitantly involved in several cardiac pathologies (*5,6*), obesity (*7*), and diabetes mellitus (*8*).

^{11}C-*meta*-Hydroxyephedrine (HED) is routinely applied in cardiac PET to assess sympathetic innervation (*9,10*). As an analog of NE, the tracer is actively recaptured into the neuron via NET, providing a quantitative indication of presynaptic sympathetic nervous integrity and function (*2,9,11*). Moreover, HED is resistant to the NE–metabolizing enzymes monoamine oxidase (MAO) and catechol-*O*-methyltransferase (*9*). Characterization studies of HED have demonstrated dependence of retention on the functionality and availability of NET (*12,13*), confirming specificity in myocardium, spleen, and adrenal glands (*9,11,14*). Pharmacokinetic studies performed in animal models and isolated organ systems (*2,9,11,15*) have implied a correlation between NE concentration and clearance rate of HED (*2,15*). Metabolite analyses in rats, guinea pigs, dogs, and humans revealed that metabolites detected in plasma and

liver are not present in cardiac tissue, facilitating qualitative image analysis and clinical interpretation (*9,11,16*).

Whereas cardiac retention of HED has been well documented and applied in several cardiovascular and autonomic disorders (*10,13,14,17,18*), uptake in other tissues with rich noradrenergic innervation remains equivocal. In this study, we analyzed the effect of treatments altering synaptic NE levels on specific retention of HED. Additionally, we examined the potential of HED to assess SNS innervation in brown adipose tissue, lung, pancreas, white adipose tissue, skeletal muscle, liver, and kidney by identifying NET-specific retention and determining the presence of radiolabeled metabolites in these tissues.

MATERIALS AND METHODS

Materials

HED was synthesized as described previously (*9*) and purified by semipreparative high-performance liquid chromatography (HPLC) using a Luna C18 column (250 × 10 mm, 10 μm, Phenomenex; 5:95 acetonitrile [MeCN]/0.1 M ammonium formate [v/v]; 7 mL/min; retention time [Rt], 7 min). After solvent removal via rotary evaporation, HED was reconstituted in 50:44:6 0.9% saline/water/8.4% sodium bicarbonate (v/v/v) before injection. High radiochemical purity (>99%) and specific activity (7.4–55.5 GBq/μmol; 400–1,500 mCi/μmol) were obtained. Desipramine hydrochloride, nisoxetine hydrochloride, metaraminol bitartrate, tranylcypromine hydrochloride, and norepinephrine bitartrate were purchased from Sigma-Aldrich and dissolved in 0.9% saline. Osmotic minipumps (Alzet 2001D) were obtained from Durect Corp. and prepared for implantation in a laminar flow fume hood. Pumps were filled to maximal capacity with dissolved NE or saline. To ensure even flow at the time of the experiment, pumps were equilibrated at 37°C for 3 h before implantation.

Animals

Animal experiments were conducted in accordance with the recommendations of the Canadian Council on Animal Care and with approval from the Animal Care Committee of the University of Ottawa. Adult male Sprague–Dawley rats (225–275 g at time of experiment) were obtained from Charles River Canada and were housed in a temperature-controlled animal facility under a 12-h light/dark cycle with food and water ad libitum.

Osmotic minipumps were implanted subcutaneously under light anesthesia (1%–2% isoflurane). Briefly, a 0.5-cm oblique incision was made lateral to the midline at the lower cervical level. A subcutaneous pocket was created using surgical scissors, the pump was inserted, and the incision was closed using surgical clips. Animals were treated with buprenorphine (0.3 mg/kg subcutaneously) 1 h before the experiment. Sham animals were implanted with a minipump containing saline using an identical surgical procedure.

Ex Vivo Biodistribution

Biodistribution studies were performed in conscious animals as described previously (*19*). Briefly, 51.8–74 MBq (1.4–2.0 mCi at time of first injection) of HED were injected as a 0.1- to 0.3-mL bolus into the lateral tail vein of each restrained rat. Tail veins were vasodilated using an infrared heat lamp to facilitate injection. In each individual experiment, all animals received approximately the same mass dose of HED (0.24–1.26 μg). Animals were sacrificed by decapitation at a defined time point after tracer injection (15, 30, 45, 60, and 90 min). A sample of trunk blood was collected into heparinized tubes. Heart, kidney, pancreas, and samples of lung, liver, intrascapular brown adipose tissue, abdominal white adipose tissue, and quadriceps femoris were rapidly excised, weighed, and counted (decay corrected) for radioactivity in a γ-counter along with 1% standard dilutions of HED injection volume. Tracer retention is expressed as the percentage of injected dose per gram of tissue (%ID/g).

Pharmacologic Studies

Drug treatments and doses were selected according to previous experiments. To evaluate NET-specific retention of HED, animals were pretreated with the NET inhibitor desipramine (10 mg/kg intraperitoneally 30 min earlier) (*9,11*) or nisoxetine (10 mg/kg intraperitoneally 30 min earlier) (*20*). Synaptic competition for neuronal reuptake was tested by coadministration of the HED precursor and NE analog metaraminol (1.3 mg/kg intravenous coinjection) (*11*). The effect of acute elevations of synaptic NE was assessed by pretreatment with the MAO inhibitor tranylcypromine (0.5–10 mg/kg intraperitoneally 1 h earlier) (*21*) or subcutaneous NE minipump infusion at 0.05, 0.15, and 0.45 mg/kg/h over 6 h after surgery (0.3, 0.9, and 2.7 mg/kg cumulative dose) (*22*). Animals were sacrificed at 30 min after tracer injection and tissues were processed as described.

HPLC Column-Switch Apparatus

A combined and modified HPLC protocol incorporating the column-switch methodology developed by Hilton et al. (*23*) and the weak cation-exchange solid-phase HED extraction reported by Link et al. (*16*) was applied to capture HED and similar protonated metabolites while eluting nonprotonated metabolites, proteins, and other macromolecules before introduction onto the analytic column. Briefly, the HPLC apparatus consisted of 2 pumps (Waters): one eluting solvent A (1:99 MeCN/water [v/v]) at 2 mL/min across the capture cartridge (Alltech Direct-Connect refillable guard column, 2 × 20 mm) packed with 50 mg of weak cation-exchange sorbent (WCX, Waters Oasis) and fitted with 2.5-μm frits (Alltech, 2-mm filter elements); and the other delivering solvent B (5:95 MeOH/aqueous 50 mM ammonium formate, 0.27 mM ethylenediaminetetraacetic acid, 0.346 mM 1-octane sulfonic acid [v/v]) at 1 mL/min across the cation-exchange analytic column (Partisil SCX, 250 × 4.6 mm, 10 μm; Phenomenex). Eluents of both columns were analyzed in series by ultraviolet (UV) absorbance detection at 280 nm (Waters 486) and coincidence radiation detection (Bioscan). Signals were integrated using the PeakSimple Six-Port Chromatography Data System (Chromatographic Specialties), analyzed using PeakSimple 3.29 software and are presented as the percentage of total noise- and decay-corrected radioactivity signal accounted for by ^{11}C-labeled metabolites (retained or unretained by the WCX resin) and by unmetabolized HED.

Samples (≤2 mL) were injected onto the capture column, allowing proteins and macromolecules to elute as measured by UV detection. After 4–5 min, column flow was then switched, delivering solvent B across the capture cartridge and eluting retained contents onto the analytic column. Under these conditions, authentic HED was retained (>99%) on the WCX sorbent (Rt, 14 min after column/solvent switch). The capture column was reactivated between runs under MeOH and water and then reequilibrated under solvent A before the next injection. Standard cation-exchange (MCX, Waters Oasis), anion-exchange (MAX,

Waters Oasis), hydrophilic lipophilic balanced (HLB, Waters Oasis), and activated alumina (type WA4, Sigma) sorbents were also tested for their ability to retain HED.

Plasma and Tissue Radiolabeled Metabolite Analysis

Restrained animals were injected with 370–444 MBq (10–12 mCi) of HED and sacrificed 30 min later. A high radioactive dose was used to analyze multiple tissues in a single animal, using the HPLC column-switch system as described to accommodate for radioactive decay. Heart ($n = 3$), brown adipose tissue ($n = 4$), and pancreas ($n = 3$) were rapidly dissected and a plasma sample ($n = 6$) was obtained from centrifuged blood (3,000*g*, 4,000 rpm, 5 min). Tissues were processed for injection on the HPLC system as described previously (*19*). Briefly, samples were homogenized in 80:20 ethanol/water (v/v) using a Polytron tissue homogenizer. Tissue homogenates were separated using an ultracentrifuge at 82,000*g* (22,000 rpm) for 15 min. Supernatant was extracted and solvent was removed by rotary evaporation. Remaining residue was reconstituted under 1:99 MeCN/water (v/v) and microfiltered at 0.22 μm (Cathivex GS) before injection and testing on HPLC. Standard control experiments ($n = 6$) were assessed for each formulation using the same procedure as described, but directly adding authentic HED to tissue or plasma before homogenization.

Statistical Analysis

Statistical comparisons were completed using 1-way ANOVA on mean retention values applying Bonferroni post hoc tests. All statistics were performed using SPSS 14.0 software (SPSS Inc.). Vehicle-treated animals did not deviate significantly from untreated controls and, therefore, were pooled for statistical analysis. Significance was considered at $P < 0.05$.

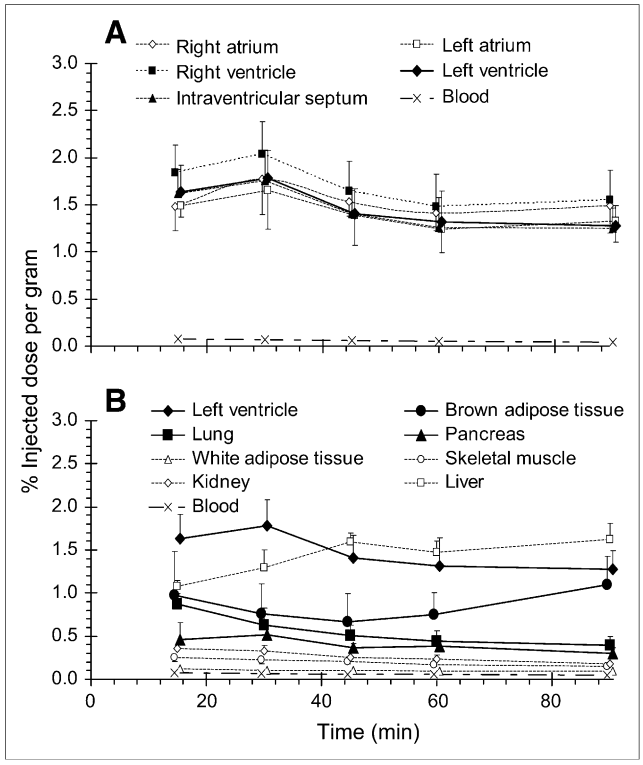

FIGURE 1. Distribution of HED in myocardium (A) and other peripheral tissues (B) at 15, 30, 45, 60, and 90 min after intravenous injection in rats. Data are shown as mean %ID/g of tissue ± SD ($n = 26$ at 30 min; $n = 6$ at 15, 45, 60, and 90 min).

RESULTS

HED Ex Vivo Retention Studies

Time-course evaluation revealed high uptake of HED in myocardial tissue that was maximal (1.66–2.04 %ID/g) at 30 min after tracer injection (Fig. 1A). Due to the relative uniformity of myocardial tracer retention, left ventricle is considered representative of the whole heart hereafter. Moderately high HED retention was also observed in brown adipose tissue, pancreas, and lung, with comparatively lower levels in white adipose tissue, skeletal muscle, and kidney (Fig. 1B). Liver uptake was considerable and surpassed heart values at 45 min after injection. Pretreatment with NET inhibitors significantly reduced tracer retention in left ventricle, brown adipose tissue, lung, and pancreas to similar levels (0.20–0.29 %ID/g). Conversely, no blockade of HED distribution was discerned in liver, skeletal muscle, kidney, or blood. Reductions of tracer retention observed after coadministration of the NE analog metaraminol followed the same tissue distribution as NET blockade (Fig. 2; Table 1). Modest reductions in tracer

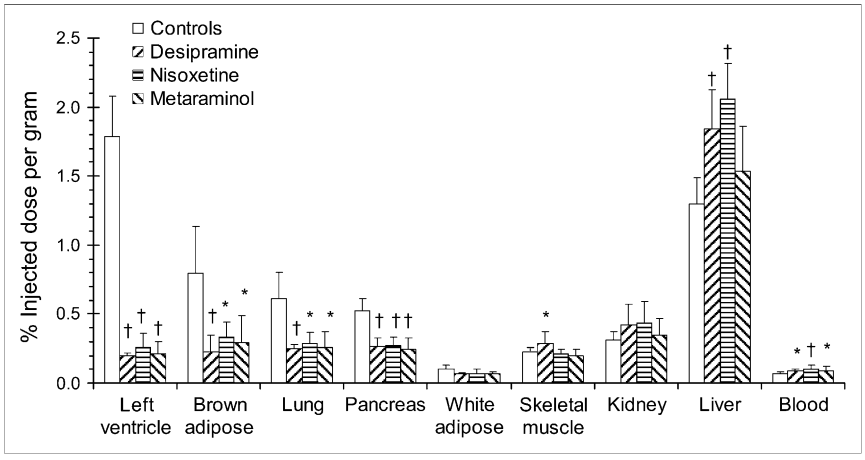

FIGURE 2. Effect of blocking NET-specific HED retention with NE reuptake inhibitor desipramine (10 mg/kg intraperitoneally 30 min earlier) or nisoxetine (10 mg/kg intraperitoneally 30 min earlier) or increasing competition for reuptake with NE analog metaraminol (1.3 mg/kg intravenous coinjection). Animals were sacrificed at 30 min after HED injection. Data are shown as mean %ID/g of tissue ± SD (controls, $n = 26$; desipramine, $n = 7$; nisoxetine, $n = 6$; metaraminol, $n = 6$); $^{\dagger}P < 0.0001$; $^{*}P < 0.05$ as compared with controls using 1-way ANOVA with Bonferroni post hoc comparisons.

TABLE 1
Percent Change in HED Uptake After Pharmacologic Treatment in Tissues Exhibiting NET-Specific Retention

Treatment and dose	Left ventricle	Brown adipose	Lung	Pancreas
Desipramine (n = 7), 10 mg/kg 30 min earlier	−89	−71	−60	−50
Nisoxetine (n = 6), 10 mg/kg 30 min earlier	−85	−57	−53	−49
Metaraminol (n = 6), 1.3 mg/kg intravenous coinjection	−88	−63	−58	−54

Percent change = ([%ID/g treated] − [%ID/g control])/(%ID/g control) × 100%.

Values presented represent significant deviation ($P < 0.05$) in %ID/g treated as compared with untreated controls.

retention observed in white adipose tissue with these treatments were not statistically significant.

Tranylcypromine or exogenous NE infused subcutaneously dose-dependently reduced HED retention in heart, brown adipose tissue, lung, pancreas, and white adipose tissue (Fig. 3; Table 2). At the highest administered doses, significant blockade of HED uptake was comparable to NET inhibition in tissues displaying specific retention. Additionally, skeletal muscle HED accumulation was consistently and significantly reduced (9%–13%) by subcutaneous infusion of NE but not by tranylcypromine treatment. No reduction in tracer retention levels after either treatment was observed in liver, kidney, or blood compared with controls (Fig. 3).

Radiolabeled Metabolite Analysis

MCX, MAX, HLB, and alumina resins were unable to retain HED in a satisfactory manner for HPLC analysis. Contrary to the MCX sorbent, which was shown to bind too strongly to the tracer, resulting in tailing of the radioactivity peak after extraction, the WCX resin provided clear adherence and elution of authentic HED (data not shown). ^{11}C-Labeled metabolites were eluted from the WCX sorbent before column and solvent switching. At 30 min after injection, 39% ± 8% of total noise- and decay-corrected radioactivity represented metabolites in plasma, whereas 61% ± 8% was unchanged HED (Fig. 4A). In contrast, predominantly unmetabolized HED was observed in heart (94% ± 2%), brown adipose tissue (95% ± 3%), and pancreas (92% ± 3%) (Figs. 4B–4D). In standard control tissue samples with authentic HED, radioactivity present

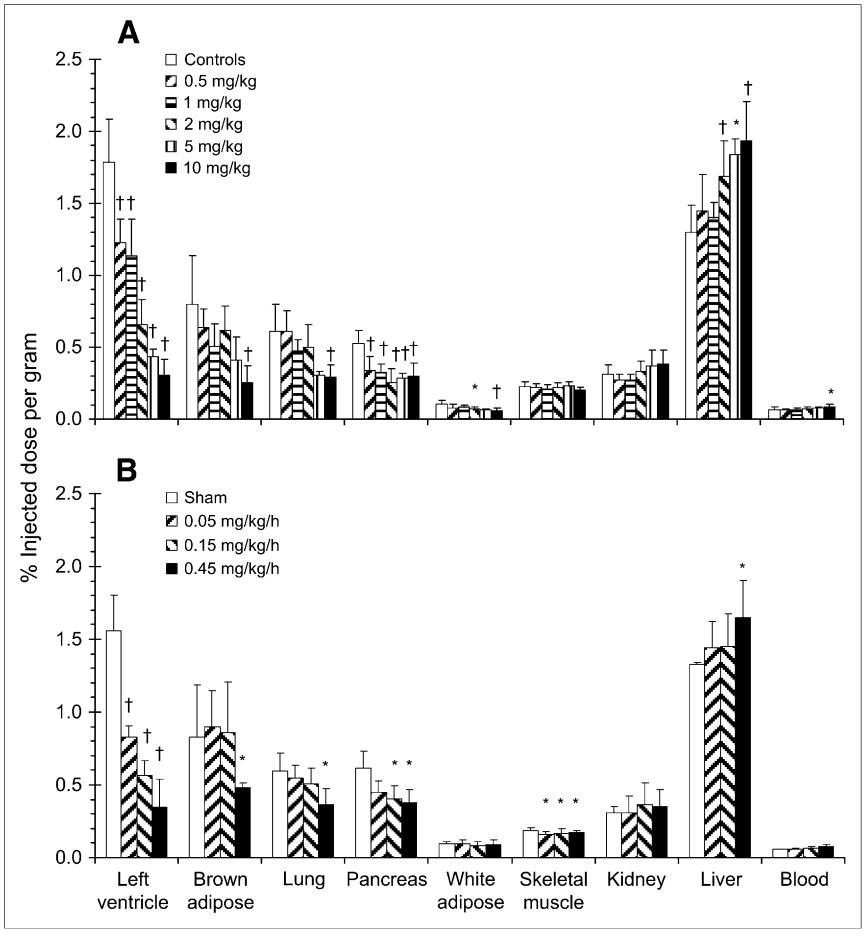

FIGURE 3. Effect of elevated NE on HED retention by pretreatment with MAO inhibitor tranylcypromine (0.5–10 mg/kg intraperitoneally 1 h earlier) (A) or subcutaneous infusion of NE (0.05–0.45 mg/kg/h, 6 h) (B). Animals were sacrificed at 30 min after HED injection. Data are shown as mean %ID/g of tissue ± SD (tranylcypromine: controls, n = 26; 0.5 mg/kg, n = 9; 1 mg/kg, n = 7; 2 mg/kg, n = 12; 5 mg/kg, n = 3; 10 mg/kg, n = 12; NE: sham, n = 8; 0.05 mg/kg/h, n = 6; 0.15 mg/kg/h, n = 10; 0.45 mg/kg/h, n = 9); $^{\dagger}P < 0.0001$; $^{*}P < 0.05$ as compared with controls using 1-way ANOVA with Bonferroni post hoc comparisons.

TABLE 2
Percent Change in HED Uptake After Pharmacologic Treatment to Elevate NE in Tissues Exhibiting NET-Specific Retention

Treatment and dose	Left ventricle	Brown adipose	Lung	Pancreas
Tranylcypromine				
0.5 mg/kg (n = 9)	−30	−20	+1	−36
1.0 mg/kg (n = 7)	−35	−36	−22	−38
2.0 mg/kg (n = 12)	−63	−22	−17	−53
5.0 mg/kg (n = 3)	−75	−48	−49	−47
10 mg/kg (n = 12)	−82	−68	−52	−44
NE				
0.05 mg/kg/h (n = 6)	−53	+13	−10	−16
0.15 mg/kg/h (n = 10)	−68	+9	−17	−23
0.45 mg/kg/h (n = 9)	−80	−40	−40	−29

Percent change = ([%ID/g treated] − [%ID/g control])/(%ID/g control) × 100%.

All values presented represent significant deviation ($P < 0.05$) in %ID/g treated as compared with untreated controls except brown adipose tissue and lung (tranylcypromine: 0.5, 1.0, 2.0, 5.0 mg/kg; NE: 0.05, 0.15 mg/kg/h) and pancreas (NE: 0.05 mg/kg/h).

was solely representative of unchanged HED (data not shown).

DISCUSSION

Previous examinations of HED retention have focused primarily on myocardium. However, the SNS is ubiquitous, forming connections throughout the body to various organ systems. The data presented here indicate that HED retention is reduced by NET blockade in myocardium by >85% and in brown adipose tissue, lung, and pancreas by 49%–71%. These results demonstrate that HED may be aptly applied in measuring SNS innervation and function in a wider array of tissues than considered previously.

Previous examinations (*9,11,12*) have shown higher %ID/g values in myocardium (2.7–3.2 %ID/g) than those reported here. Law et al. demonstrated a slight reduction in myocardial radioactivity when HED was coinjected with 10 nmol/kg (2.2 μg/kg) unlabeled compound (*11*). In the present study, the injected doses of HED overlap this mass dose (0.9–5.6 μg/kg), which may account for the lower uptake observed in myocardium and reduce the apparent uptake in other tissues as well.

Whereas a high signal is consistently detected in the heart, specific HED retention at lower levels has been reported previously in the spleen, adrenal glands, and lungs (*9,11*). Indeed, binding assays using selective NET inhibitors ^{3}H-mazindol and ^{3}H-desipramine have demonstrated NET densities as high as 250–500 fmol/mg protein in myocardium (*12,13,24*). As the vast majority of NE used by the heart is synthesized within cardiac sympathetic neurons (*25*), there is less dependence on circulating NE levels, and recapture of neurotransmitter is critical for normal cardiac function. The majority of research on HED has demonstrated that higher tracer uptake directly correlates with higher NET density (*2,12,13,26*). The observation of lower HED retention in the lungs as compared with the heart supports earlier reports (*9,11*). By contrast, the selective NET inhibitor (*R,R*)-^{11}C-methyl-reboxetine displayed similar binding levels for lung and heart (*27*). This apparently high lung uptake of (*R,R*)-^{11}C-methyl-reboxetine may result from the greater lipophilicity and, hence, nonspecific binding of this tracer in comparison with HED.

The presence of NET-specific HED retention in adipose tissue reflects a regulated network of NE synapses controlling lipolytic and thermogenic pathways. Unlike white adipocytes, brown adipose tissue exhibits a greater degree of sympathetic innervation as well as blood supply, owing to its dynamic involvement in both energy homeostasis and lipid clearance (*3,28*). NET densities in rat intrascapular brown adipose tissue have been estimated at 1,700 fmol/mg protein, as determined with ^{3}H-nisoxetine (*29*). This higher value may derive from the lower proportion of protein within adipocytes as compared with cardiomyocytes (*3*). In general, previous work has reported that NET is regulated in parallel with postsynaptic β-adrenoceptors (*24*). Ungerer et al. demonstrated a correlation between the density of adrenoceptors and NET, as determined by the nonselective β-adrenoceptor antagonist ^{3}H-CGP12177 and ^{3}H-mazindol binding, respectively, suggesting that β-adrenoceptor density may provide a useful proxy measurement of NET expression (*13*). Accordingly, brown adipose tissue β-adrenoceptor density has been shown to be two thirds of myocardial levels (*28*), a ratio that is closely reflected by the current HED measurements at 30 min after injection. Pancreatic ducts have been shown to contain the majority of NE in the pancreas, indicating that SNS control is not directly acting on the heavier secretory cells (*30*). The degree of NET and adrenoceptor expression in pancreatic ductile cells remains contentious.

Lack of specific tracer accumulation in skeletal muscle, kidney, and liver after NET blockade has been reported here and elsewhere (*11*). A greater dispersal of NET and wider synaptic clefts in skeletal muscle may render blockade of reuptake ineffective (*1*). Studies with the highly selective NET inhibitor sibutramine have suggested that doses capable of elevating NE in the heart do not significantly affect NE levels or vasoconstriction in skeletal muscle (*31*). ^{3}H-NE uptake assays have shown slowed uptake in kidney as compared with heart (*26*), which may suggest reduced or diffuse NET expression, though quantitative values for kidney have not been reported to our knowledge.

Interestingly, nonspecific retention of HED as determined by NET blockade is comparable among heart, brown adipose tissue, lung, and pancreas and aligns with total retention in skeletal muscle and kidney, where only nonspecific retention is observed. This uniformity indicates that tissue differences in total HED accumulation likely derive

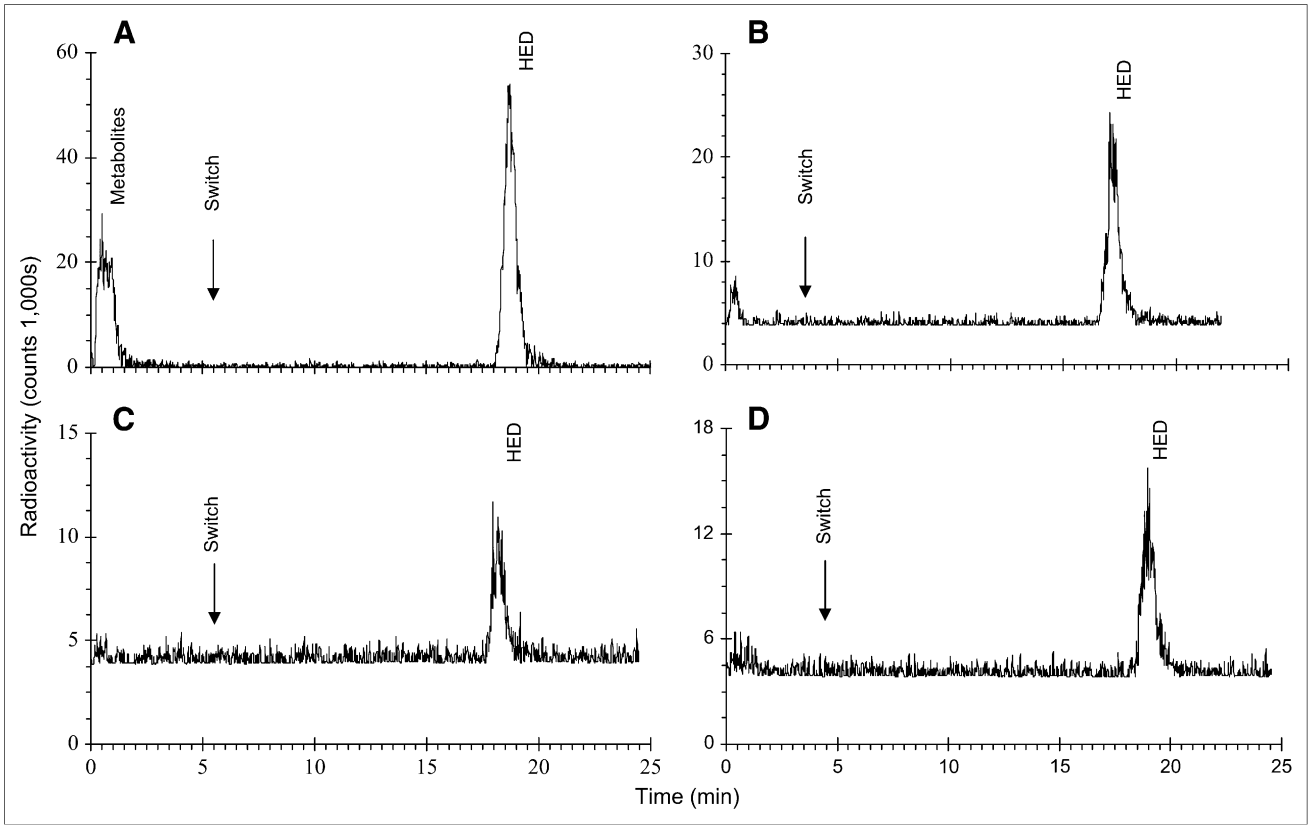

FIGURE 4. Representative HPLC chromatograms of ^{11}C-labeled peaks at 30 min after HED injection in plasma (A), heart (B), brown adipose tissue (C), and pancreas (D). Column and solvents were switched 4–5 min after injection onto HPLC; unchanged HED was eluted at 14 min after column/solvent switch. Radioactivity levels represent total counts and vary, depending on time of analysis due to isotope decay.

from NET-specific uptake of the tracer, reflecting differential SNS neuronal density or NET expression.

Elevations of endogenous NE (via tranylcypromine) or exogenous NE (subcutaneous infusion) reduced myocardial, brown adipose tissue, lung, pancreatic, and, to a lesser extent, white adipose retention of HED in a dose-dependent manner. Tranylcypromine treatment has been reported to increase tissue NE levels by 60% within 1 h of administration (*32*), evoke elevations of blood pressure and heart rate (*33*), and increase the cache of endogenous neuronal NE stores (*34*). Additionally, tranylcypromine has low affinity for NET (inhibitory constant [k_i] = 5 μM) (*35*). Despite this, direct inhibition of the transporter is not anticipated at the low doses used in the present study that nevertheless evoked significant reductions of cardiac HED retention. Similar results were obtained with the NE analog metaraminol, as reported here and elsewhere (*11*). Studies in isolated perfused rat hearts have suggested that although initial HED uptake is unhindered, clearance is hastened in the presence of NE (*2,15*), a result that is supported by our data. Subcutaneous infusion of NE has been shown to elevate tissue (synaptic) and plasma levels of the neurotransmitter (*24*). Moderately lower HED retention in skeletal muscle observed following NE infusion—but not with MAO inhibition, NET inhibition, or metaraminol treatment—suggests that a nonspecific mechanism such as NE-induced vasoconstriction may contribute to a global reduction in tracer uptake due to diminished delivery (*36*). However, the decrease in skeletal muscle HED uptake (9%–13%) is minor compared with the reductions obtained in tissues exhibiting specific retention, implying that perfusion may only partially explain the NE results. Taken together, the tranylcypromine, NE, and metaraminol results strongly suggest that enhanced synaptic NE significantly reduces HED retention by competitive reuptake, decreased neuronal storage capacity, or increased vesicle release.

The capture of physiologically protonated HED and metabolites by weak cation-exchange resin in the presence of a saline gradient has been reported previously (*16*). We have demonstrated the ability to adhere protonated HED to weak cation-exchange sorbent without a saline gradient using the HPLC column-switch approach (*23*). Metabolite analyses in rats, guinea pigs, dogs, and humans indicated that at 30 min after HED administration, metabolites represent 30%–50% of total radioactivity in plasma, with no labeled metabolites present in myocardium (*9,11,16*). We report here that, like the heart, there is an absence of ^{11}C-labeled metabolites in brown adipose tissue and pancreas. This property, in combination with the presence of NET-specific HED retention, facilitates PET image analysis and

may allow the application of existing cardiac retention models to pancreas and brown adipose tissue.

Clinical applications of HED PET have included cardiovascular disorders such as acute myocardial infarction (*14*), congestive heart failure (*10,17*), dilated cardiomyopathies (*13*), multivessel coronary artery disease (*5*), and Brugada syndrome ventricular fibrillation (*18*), as well as the systemic disorders pheochromocytoma (*37*), diabetes mellitus (*8*), and parkinsonian syndromes such as multisystem atrophy (*38*). Imaging of brown adipose tissue, lung, and pancreas present unique and formidable challenges because of problems in localization and signal identification for brown adipose tissue (*3*), low in vivo tissue density hindering acquisition of high-contrast images for lung (*21*), and nonpancreatic abdominal uptake causing poor signal-to-noise ratios for pancreas (*39*). Recent use of ^{18}F-FDG in full-body scanning has revealed anomalous tracer uptake in areas of supraclavicular fat (*40*), suggesting that isolation of brown adipose tissue in large mammals may be possible. Although lung tissue density remains a problem for neurohormonal imaging, the advent of fused PET/CT technology may circumvent some of the other challenges to noncardiac imaging, allowing CT delineation of brown adipose tissue or pancreas for subsequent PET evalutations.

CONCLUSION

In addition to the heart, NET-specific uptake of HED without labeled metabolites is observed in lung, pancreas, and brown adipose tissue, supporting the potential for novel imaging of SNS integrity in various metabolic disease states. Moreover, the present study strongly suggests an inverse correlation between tracer retention and synaptic NE dependent on the presence of NET-specific retention of HED.

ACKNOWLEDGMENTS

The authors acknowledge the contributions of the University of Ottawa Heart Institute Cardiac PET Centre Radiochemistry staff (Samantha Mason, Jeffrey Collins, and Paul Coletta) for radiochemical synthesis; thank Miran Kenk and Stephanie Thorn for assistance with both the manuscript and the biodistribution metabolite analysis studies; and also thank Michael Greene, Maryam Parsa-Nezhad, and the Ottawa Heart Institute Animal Care and Veterinary Staff for general assistance with the experiments. This work is partially supported by an Ontario Graduate Scholarship in Science and Technology.

REFERENCES

1. Esler M, Jennings G, Lambert G, Meredith I, Horne M, Eisenhofer G. Overflow of catecholamine neurotransmitters to the circulation: source, fate, and functions. *Physiol Rev.* 1990;70:963–985.
2. Raffel DM, Wieland DM. Assessment of cardiac sympathetic nerve integrity with positron emission tomography. *Nucl Med Biol.* 2001;28:541–559.
3. Collins S, Surwit RS. The beta-adrenergic receptors and the control of adipose tissue metabolism and thermogenesis. *Recent Prog Horm Res.* 2001;56:309–328.
4. Noble MD, Liddle RA. Neurohormonal control of exocrine pancreatic secretion. *Curr Opin Gastroenterol.* 2005;21:531–537.
5. Bulow HP, Stahl F, Lauer B, et al. Alterations of myocardial presynaptic sympathetic innervation in patients with multi-vessel coronary artery disease but without history of myocardial infarction. *Nucl Med Commun.* 2003;24:233–239.
6. Meredith IT, Broughton A, Jennings GL, Esler MD. Evidence of a selective increase in cardiac sympathetic activity in patients with sustained ventricular arrhythmias. *N Engl J Med.* 1991;325:618–624.
7. Bachman ES, Dhillon H, Zhang CY, et al. βAR signaling required for diet-induced thermogenesis and obesity resistance. *Science.* 2002;297:843–845.
8. Stevens MJ, Raffel DM, Allman KC, Schwaiger M, Wieland DM. Regression and progression of cardiac sympathetic dysinnervation complicating diabetes: an assessment by C-11 hydroxyephedrine and positron emission tomography. *Metabolism.* 1999;48:92–101.
9. Rosenspire KC, Haka MS, Van Dort ME, et al. Synthesis and preliminary evaluation of carbon-11-meta-hydroxyephedrine: a false transmitter agent for heart neuronal imaging. *J Nucl Med.* 1990;31:1328–1334.
10. Link JM, Stratton JR, Levy W, et al. PET measures of pre- and post-synaptic cardiac beta adrenergic function. *Nucl Med Biol.* 2003;30:795–803.
11. Law MP, Osman S, Davenport RJ, Cunningham VJ, Pike VW, Camici PG. Biodistribution and metabolism of [N-methyl-^{11}C]m-hydroxyephedrine in the rat. *Nucl Med Biol.* 1997;24:417–424.
12. Raffel DM, Chen W, Sherman PS, Gildersleeve DL, Jung YW. Dependence of cardiac ^{11}C-meta-hydroxyephedrine retention on norepinephrine transporter density. *J Nucl Med.* 2006;47:1490–1496.
13. Ungerer M, Hartmann F, Karoglan M, et al. Regional in vivo and in vitro characterization of autonomic innervation in cardiomyopathic human heart. *Circulation.* 1998;97:174–180.
14. Allman KC, Wieland DM, Muzik O, Degrado TR, Wolfe ER Jr, Schwaiger M. Carbon-11 hydroxyephedrine with positron emission tomography for serial assessment of cardiac adrenergic neuronal function after acute myocardial infarction in humans. *J Am Coll Cardiol.* 1993;22:368–375.
15. DeGrado TR, Hutchins GD, Toorongian SA, Wieland DM, Schwaiger M. Myocardial kinetics of carbon-11-meta-hydroxyephedrine: retention mechanisms and effects of norepinephrine. *J Nucl Med.* 1993;34:1287–1293.
16. Link JM, Synovec RE, Krohn KA, Caldwell JH. High speed liquid chromatography of phenylethanolamines for the kinetic analysis of [^{11}C]-meta-hydroxyephedrine and metabolites in plasma. *J Chromatogr B Biomed Sci Appl.* 1997;693:31–41.
17. Vesalainen RK, Pietila M, Tahvanainen KU, et al. Cardiac positron emission tomography imaging with [^{11}C]hydroxyephedrine, a specific tracer for sympathetic nerve endings, and its functional correlates in congestive heart failure. *Am J Cardiol.* 1999;84:568–574.
18. Kies P, Wichter T, Schafers M, et al. Abnormal myocardial presynaptic norepinephrine recycling in patients with Brugada syndrome. *Circulation.* 2004;110:3017–3022.
19. Lourenco CM, Houle S, Wilson AA, DaSilva JN. Characterization of (*R*)-[^{11}C]rolipram for PET imaging of phosphodiesterase-4: in vivo binding, metabolism, and dosimetry studies in rats. *Nucl Med Biol.* 2001;28:347–358.
20. Wong DT, Threlkeld PG, Best KL, Bymaster FP. A new inhibitor of norepinephrine uptake devoid of affinity for receptors in rat brain. *J Pharmacol Exp Ther.* 1982;222:61–65.
21. Lourenco CM, Kenk M, Beanlands RS, DaSilva JN. Increasing synaptic noradrenaline, serotonin and histamine enhances in vivo binding of phosphodiesterase-4 inhibitor (R)-[^{11}C]rolipram in rat brain, lung and heart. *Life Sci.* 2006;79:356–364.
22. Laycock SK, Kane KA, McMurray J, Parratt JR. Captopril and norepinephrine-induced hypertrophy and haemodynamics in rats. *J Cardiovasc Pharmacol.* 1996;27:667–672.
23. Hilton J, Yokoi F, Dannals RF, Ravert HT, Szabo Z, Wong DF. Column-switching HPLC for the analysis of plasma in PET imaging studies. *Nucl Med Biol.* 2000;27:627–630.
24. Mardon K, Montagne O, Elbaz N, et al. Uptake-1 carrier downregulates in parallel with the beta-adrenergic receptor desensitization in rat hearts chronically exposed to high levels of circulating norepinephrine: implications for cardiac neuroimaging in human cardiomyopathies. *J Nucl Med.* 2003;44:1459–1466.
25. Kopin IJ, Gordon EK. Origin of norepinephrine in the heart [letter]. *Nature.* 1963;199:1289.
26. Liang CS, Fan TH, Sullebarger JT, Sakamoto S. Decreased adrenergic neuronal uptake activity in experimental right heart failure: a chamber-specific contributor to beta-adrenoceptor downregulation. *J Clin Invest.* 1989;84:1267–1275.
27. Ding YS, Lin KS, Garza V, et al. Evaluation of a new norepinephrine transporter PET ligand in baboons, both in brain and peripheral organs. *Synapse.* 2003;50:345–352.

28. Raasmaja A, York DA. Alpha 1- and beta-adrenergic receptors in brown adipose tissue of lean (Fa/?) and obese (fa/fa) Zucker rats: effects of cold-acclimation, sucrose feeding and adrenalectomy. *Biochem J.* 1988;249:831–838.
29. King VL, Dwoskin LP, Cassis LA. Cold exposure regulates the norepinephrine uptake transporter in rat brown adipose tissue. *Am J Physiol.* 1999;276:R143–R151.
30. Yi E, Smith TG, Baker RC, Love JA. Catecholamines and 5-hydroxytryptamine in tissues of the rabbit exocrine pancreas. *Pancreas.* 2004;29:218–224.
31. Birkenfeld AL, Schroeder C, Boschmann M, et al. Paradoxical effect of sibutramine on autonomic cardiovascular regulation. *Circulation.* 2002;106: 2459–2465.
32. Routledge C, Marsden CA. Comparison of the effects of selected drugs on the release of hypothalamic adrenaline and noradrenaline measured in vivo. *Brain Res.* 1987;426:103–111.
33. Keck PE Jr, Carter WP, Nierenberg AA, Cooper TB, Potter WZ, Rothschild AJ. Acute cardiovascular effects of tranylcypromine: correlation with plasma drug, metabolite, norepinephrine, and MHPG levels. *J Clin Psychiatry.* 1991;52:250–254.
34. Fillenz M, Stanford SC. Vesicular noradrenaline stores in peripheral nerves of the rat and their modification by tranylcypromine. *Br J Pharmacol.* 1981;73:401–404.
35. Raffel DM, Chen W. Binding of [^{3}H]mazindol to cardiac norepinephrine transporters: kinetic and equilibrium studies. *Naunyn Schmiedebergs Arch Pharmacol.* 2004;370:9–16.
36. Pop-Busui R, Kirkwood I, Schmid H, et al. Sympathetic dysfunction in type 1 diabetes: association with impaired myocardial blood flow reserve and diastolic dysfunction. *J Am Coll Cardiol.* 2004;44:2368–2374.
37. Shulkin BL, Wieland DM, Schwaiger M, et al. PET scanning with hydroxyephedrine: an approach to the localization of pheochromocytoma. *J Nucl Med.* 1992;33:1125–1131.
38. Berding G, Schrader CH, Peschel T, et al. [N-methyl ^{11}C]meta-Hydroxyephedrine positron emission tomography in Parkinson's disease and multiple system atrophy. *Eur J Nucl Med Mol Imaging.* 2003;30:127–131.
39. Clark PB, Gage HD, Brown-Proctor C, et al. Neurofunctional imaging of the pancreas utilizing the cholinergic PET radioligand [^{18}F]4-fluorobenzyltrozamicol. *Eur J Nucl Med Mol Imaging.* 2004;31:258–260.
40. Cohade C, Osman M, Pannu HK, Wahl RL. Uptake in supraclavicular area fat ("USA-fat"): description on ^{18}F-FDG PET/CT. *J Nucl Med.* 2003;44: 170–176.